

Geophysical Research Letters®

RESEARCH LETTER

10.1029/2021GL094287

Key Points:

- Choice of sea ice thermodynamics does not lead to large differences in sea ice state due to compensating thermodynamic changes
- Antarctic Bottom Water production increases by 0.5 Sv and upper ocean becomes denser due to increasing salinity with mushy thermodynamics
- Wintertime air-sea fluxes, atmospheric low-level mixing, and low cloud cover all decrease with mushy thermodynamics

Supporting Information:

Supporting Information may be found in the online version of this article.

Correspondence to:

A. K. DuVivier,
duvivier@ucar.edu







Citation:

DuVivier, A. K., Holland, M. M., Landrum, L., Singh, H. A., Bailey, D. A., & Maroon, E. A. (2021). Impacts of sea ice mushy thermodynamics in the Antarctic on the coupled Earth system. *Geophysical Research Letters*, 48, e2021GL094287. <https://doi.org/10.1029/2021GL094287>

Received 10 MAY 2021

Accepted 25 AUG 2021

Impacts of Sea Ice Mushy Thermodynamics in the Antarctic on the Coupled Earth System

A. K. DuVivier¹ , M. M. Holland¹ , L. Landrum¹ , H. A. Singh² , D. A. Bailey¹ , and E. A. Maroon³ 

¹National Center for Atmospheric Research, Boulder, CO, USA, ²School of Earth and Ocean Sciences, University of Victoria, Victoria, BC, Canada, ³Department of Atmospheric and Oceanic Sciences, University of Wisconsin, Madison, WI, USA

Abstract We analyze two preindustrial experiments from the Community Earth System Model version 2 to characterize the impact of sea ice physics on differences in coastal sea ice production around Antarctica and the resulting impact on the ocean and atmosphere. The experiment in which sea ice is a more realistic “mushy” mixture of solid ice and brine has a substantial increase in coastal sea ice frazil and snow ice production that is accompanied by decreasing bottom ice growth and increasing bottom melt. The more realistic “mushy” physics leads to an increase in water mass formation at denser water classes due primarily to surface ice processes. As a result, the subsurface ocean is denser, saltier, and there is an increase in Antarctic Bottom Water formation of ~0.5 Sv. For the atmosphere, “mushy” ice physics leads to decreased turbulent heat flux and low level cloud cover near the Antarctic coast.

Plain Language Summary We analyze experiments from the Community Earth System Model to better understand the impacts of representing sea ice as a mixture of salty water and solid ice rather than just solid ice. We focus on sea ice produced around the Antarctic coasts and find that the ways in which the sea ice grow and melt change with the two representations of sea ice, but the differences compensate so that the average sea ice state is minimally changed. However, the near surface ocean water is denser in the experiment with sea ice represented by a mix of solid ice and salty water, mainly because the ocean is saltier due to surface sea ice processes. This leads to increased formation of dense Antarctic Bottom Water. In addition, there is less energy input into the atmosphere and less low level cloud cover around the Antarctic coasts in the experiment with the sea ice represented as a mix of salty water and solid ice. Thus, there are important impacts on the Earth system based solely on the way sea ice is represented.

1. Introduction

Cold, downslope winds push sea ice away from the Antarctic coast, creating coastal polynyas—areas of open ocean surrounded by sea ice (Massom et al., 1998; Morales Maqueda, 2004). There is elevated coastal sea ice production within polynyas (Tamura et al., 2016), and satellite estimates indicate wintertime active ice production over 50% of the time (Nakata et al., 2021). While coastal polynyas make up only 1% of the sea ice area, they produce 10% of the total Antarctic sea ice (Mohrmann et al., 2021). In addition to being sea ice “factories,” polynyas are a source of heat and moisture to the atmosphere (Carrasco et al., 2003; Knuth & Cassano, 2014), a location of brine rejection necessary for formation of Antarctic Bottom Water (AABW) (Fusco et al., 2009; Kern & Aliani, 2011), and impact Southern Ocean ecology at all levels from primary productivity to top predators (Arrigo & van Dijken, 2003; Arrigo et al., 2015; Karnovsky et al., 2007; Labrousse et al., 2019). Therefore, understanding polynyas and their impacts on the coupled Earth system is important for a full understanding of the physical-biological Southern Ocean system.

A recent analysis indicates that the Community Earth System Model version 2 (CESM2) simulates reasonable coastal polynya area as compared to satellite observations (Mohrmann et al., 2021). Analysis of CESM2 experiments that differ only with respect to the sea ice thermodynamics show that sea ice thermodynamics have a small impact on the Antarctic hemispheric mean sea ice state (Bailey et al., 2020), and there are significant increases in coastal ice production for CESM2 as compared with an earlier model version (Singh et al., 2020). The incorporation of more realistic sea ice salinity processes is particularly relevant for the

Antarctic because the sea ice pack is seasonal and melts and re-grows each year (Handcock & Raphael, 2020), so representing realistic sea ice salinity processes particularly for new ice will strongly impact the Antarctic.

Motivated by the importance of Antarctic coastal sea ice on the physical and biological systems, this study expands on Bailey et al. (2020) and Singh et al. (2020) by performing analysis of the coastal sea ice mass budget and driving processes in CESM2. Our focus is on better understanding the impact of more realistic sea ice physical processes on the coupled Earth system and the potential for global impacts due to these localized sea ice processes as well as the limitations of the current coupling framework as coupled Earth system model physics evolves and becomes more realistic.

2. Data and Methods

2.1. Model Experiments

Antarctic sea ice is known to have substantial internal variability (Landrum et al., 2012), so we analyze two 100-year preindustrial (constant 1850 forcing) fully coupled CESM2 model experiments that differ only with respect to the sea ice thermodynamics. As described in detail by Danabasoglu et al. (2020), CESM2 uses the CICE version 5 thermodynamic-dynamic sea ice model component with an ice thickness distribution (Hunke et al., 2015) with a salinity dependent freezing temperature (Assur, 1958). We focus on the coastal regions (see Figures 1a–1c) because of their importance in sea ice production. The CESM2 experiments both have nominal 1° resolution, which is relevant for the fidelity of the model's representation of coastal areas.

We refer to the two CESM2 experiments, both of which use the CESM2 model code, as BL99 and MUSHY. Both thermodynamics schemes assume that sea ice is a mixture of liquid brine and solid ice but they differ in their ice salinity and melt/growth processes. BL99 is the more simplified sea ice thermodynamics and uses a fixed vertical salinity profile (Bitz & Lipscomb, 1999), while MUSHY is a more realistic thermodynamics scheme based off of laboratory and field experiments (Notz, 2005; Notz & Worster, 2008) that includes processes necessary for a time-varying vertical salinity profile (Turner & Hunke, 2015; Turner et al., 2013). Consistent with previous modeling studies (Bailey et al., 2020; Turner & Hunke, 2015) and observed Antarctic sea ice salinity profiles (Eicken, 1992; Turner & Hunke, 2015), MUSHY has higher wintertime sea ice bulk salinity (Figure S1) and the ice has highest salinity near the coast where the newest ice is formed. The saltier ice in MUSHY means the brine content is higher.

Of note, the ice salinity described above only affects internal sea ice properties and processes and is not used in the ice-ocean coupling. In CESM2 the ice-ocean exchanges use a virtual salt flux which assumes that the ice has a salinity of 4 g kg⁻¹. Therefore, the sea ice processes that reject or uptake brine and thereby affect sea ice salinity do not explicitly influence the ocean salinity. Instead, the ice-ocean salt and freshwater exchange are directly related to the changes in ice volume. This is an important limitation in the current model, but this approach to the ice-ocean coupling is consistent with other state-of-the-art Earth-system-models (see model descriptions in Keen et al., 2021). However, it is clearly unrealistic and does not take full advantage of the improved sea ice salinity processes available in MUSHY. As discussed further in the results section, this can lead to some counter-intuitive coupled impacts. Partly as a result of the insights gained from this study, work is underway to model true ice-ocean salt coupling in future versions of CESM2.

A more detailed description of the CESM2 experiments, ice-ocean coupling, and differences between MUSHY and BL99 physical processes can be found in the Supporting Information S1.

2.2. Water Mass Transformation

Following the methods of Bryan et al. (2006) and Large and Nurser (2001), we assess how MUSHY and BL99 affect the ocean's meridional overturning circulation (MOC) by calculating the surface-forced water mass transformation in isopycnal space (Groeskamp et al., 2019; Speer & Tziperman, 1992; Walin, 1982). Transformation is the rate at which water masses become lighter or denser, which at the upper boundary, occurs due to air-ocean, land-ocean, and ice-ocean fluxes of heat and freshwater. Through mass continuity, the convergence of transformation (i.e., the water mass formation) from all diapycnal processes must balance isopycnal transport in steady state. Surface-forced MOC changes can thus be attributed to individual processes that heat or freshen isopycnal outcrops. For example, if densifying processes (e.g., surface cooling,

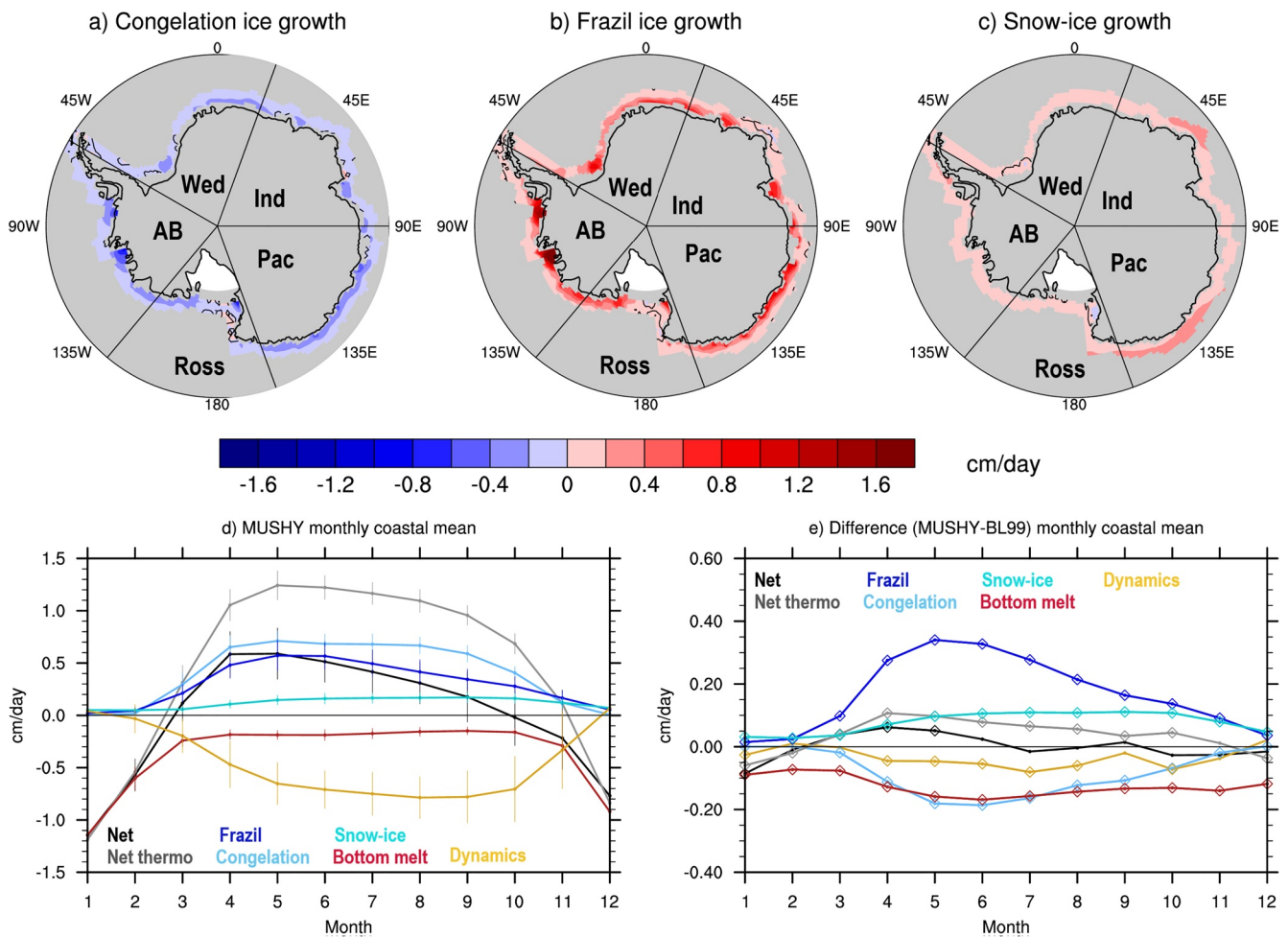


Figure 1. Winter (April-September) mean difference of (a) bottom ice growth, (b) frazil growth, and (c) snow-ice growth; regions that are significantly different at the 95% confidence level do not have stippling. (d) MUSHY mean and (e) difference in monthly coastal mean mass budget terms—Net ice growth/melt (black), net thermodynamic ice growth/melt (gray), frazil growth (dark blue), bottom ice growth (light blue), snow-ice growth (teal), bottom melt (red), and dynamics (gold). Mean budget terms include two standard deviations and differences significant at the 95% confidence level have a diamond marker. All differences show MUSHY minus BL99 and units are cm day^{-1} . Panels a, b, and c are labeled by region—Weddell Sea (Wed), Indian Ocean (Ind), Pacific Ocean (Pac), Ross Sea (Ross), and Amundsen-Bellinghousen Sea (AB).

evaporation, sea ice formation) lead to volume convergence in a density class, then subduction of that water mass occurs. Here, we assess only the surface-forced component of formation in the Antarctic coastal region, dividing it into the parts from surface heat and freshwater fluxes. The freshwater piece is further decomposed into atmospheric and land freshwater fluxes and sea ice processes. Past studies have used this approach in the Southern Ocean to determine that sea ice processes are important for the upper branch of the MOC (Abernathy et al., 2016) and that small-scale sea ice processes can strongly impact ocean water transformation (Newsom et al., 2016). In this analysis, we set density classes to 0.1 kg m^{-3} width and use potential density anomaly referenced to 2,000 dbar (σ_2) for direct comparison to the isopycnal overturning (see Supporting Information S1 for more information). Note that for comparisons of the ocean state we use potential density referenced to the surface (σ_0).

3. Results

3.1. Coastal Sea Ice Differences

Consistent with Bailey et al. (2020), we find that year-round MUSHY and BL99 differences in sea ice area and volume are small along the coast but that MUSHY has slightly higher ice concentrations and ice thick-

nesses (Figures S2–S4). The largest ice state differences are in the Amundsen-Bellingshausen Sea, and MUSHY has slightly higher sea ice volume variability in the Amundsen-Bellingshausen Sea and Indian Ocean sectors where MUSHY also has greater ice volume (Figure S4).

Despite small ice state differences, there are significant differences in coastal sea ice thermodynamic processes between the experiments (Figures 1 and S5). The differences in coastal processes compensate such that the mean sea ice state in MUSHY and BL99 is similar. Examining thermodynamic processes alone, we find that in MUSHY there is a significant increase in winter ice growth due to the large increase in frazil and snow-ice growth in MUSHY. In opposition to the increases in growth, MUSHY has decreases in bottom ice growth and increases in bottom melt (Figure 1). The overall increase in wintertime net thermodynamic ice growth in MUSHY is relevant to the freshwater exchange with the ocean. For MUSHY, the increase in thermodynamic growth is compensated by increased dynamical ice loss (Figures 1e and S6), or export from the coastal region, such that the net coastal mass budget is only significantly different in the early freeze up period (Figure 1e), which can explain the slightly higher ice concentrations and thicknesses in MUSHY (Figure S2).

3.2. Impacts on the Ocean

There are significant differences in the mean ocean response to the difference in sea ice thermodynamics and dominant ice growth processes. The MUSHY experiment has greater winter potential density (σ_0) and salinity originating at the surface along the coast and propagating downward (Figures 2d, 2e, S7, and S8). In contrast, the differences in winter temperature are small and generally statistically insignificant near the surface and coast, but there tends to be warming below the mixed layer (Figures 2f and S9). The increases in density and salinity are consistent in all sectors at depth (Figures 2g and 2h). These increases in density are primarily related to the increase in salinity as the ocean temperature is either slightly warmer, which would act to lower density, in MUSHY or statistically insignificantly different.

There is a change in water mass formation and the MOC between the two experiments as a result of the coastal sea ice process differences. In both experiments, positive formation occurs in water masses denser than 36.6 kg m^{-3} and negative formation for water masses from 35.6 to 36.6 kg m^{-3} (Figures 3a and 3b). The formation is primarily due to the freshwater removal from ice freezing for both experiments (Figure S10). The difference in formation in the two experiments is due to surface sea ice processes increasing both the surface density and the surface density fluxes in MUSHY. Within the range of positive-formation density classes ($\geq 36.6 \text{ kg m}^{-3}$), the distribution of formation shifts toward higher density classes because the near-coastal surface density is higher in MUSHY (Figures 3a and 3b). The greater area of dense outcrops in MUSHY, however, is not the sole reason for the changes: MUSHY has greater total positive formation than BL99. The sum of formation in all positive-formation density classes ($\geq 36.6 \text{ kg m}^{-3}$) is larger in MUSHY than BL99, indicating increased surface density fluxes. The increased surface fluxes in MUSHY are due to those from sea ice processes, mostly at 37.0 – 37.2 kg m^{-3} (Figure 3b), with smaller contributions from the surface heat flux and atmospheric and land freshwater fluxes. As with the mean states of both experiments, freshwater removal due to ice freezing also contributes the most to the formation difference between MUSHY and BL99 (Figure S10). The freshwater removal differs between the two experiments because of the larger ice volume production in MUSHY. Over the full Southern Ocean the differences in water mass formation (Figure S11) are similar to those in just the coastal region, as well as to those found by Abernathey et al. (2016).

The maximum subduction in the MOC occurs at the same latitude (69°S) in both experiments (Figure 3c). However, in MUSHY the MOC has weakened for densities $\sigma_2 = 36.4$ – 36.9 kg m^{-3} , but strengthens for densities $\sigma_2 = 37.0$ – 37.2 kg m^{-3} and $\sigma_2 = 37.4$ – 37.6 kg m^{-3} (Figure 3d). Similar to the formation differences in these density classes, MOC streamfunction at 69°S both strengthens and shifts to denser water classes in MUSHY. As a result, there is a small but statistically significant increase in annual mean AABW (taken here as $\sigma_2 > 37.0 \text{ kg m}^{-3}$) formation by about 0.5 Sv and weaker formation of less dense water masses (Figure 3e). These overturning differences qualitatively correspond to the coastal surface-forced water mass formation changes in the same density classes.

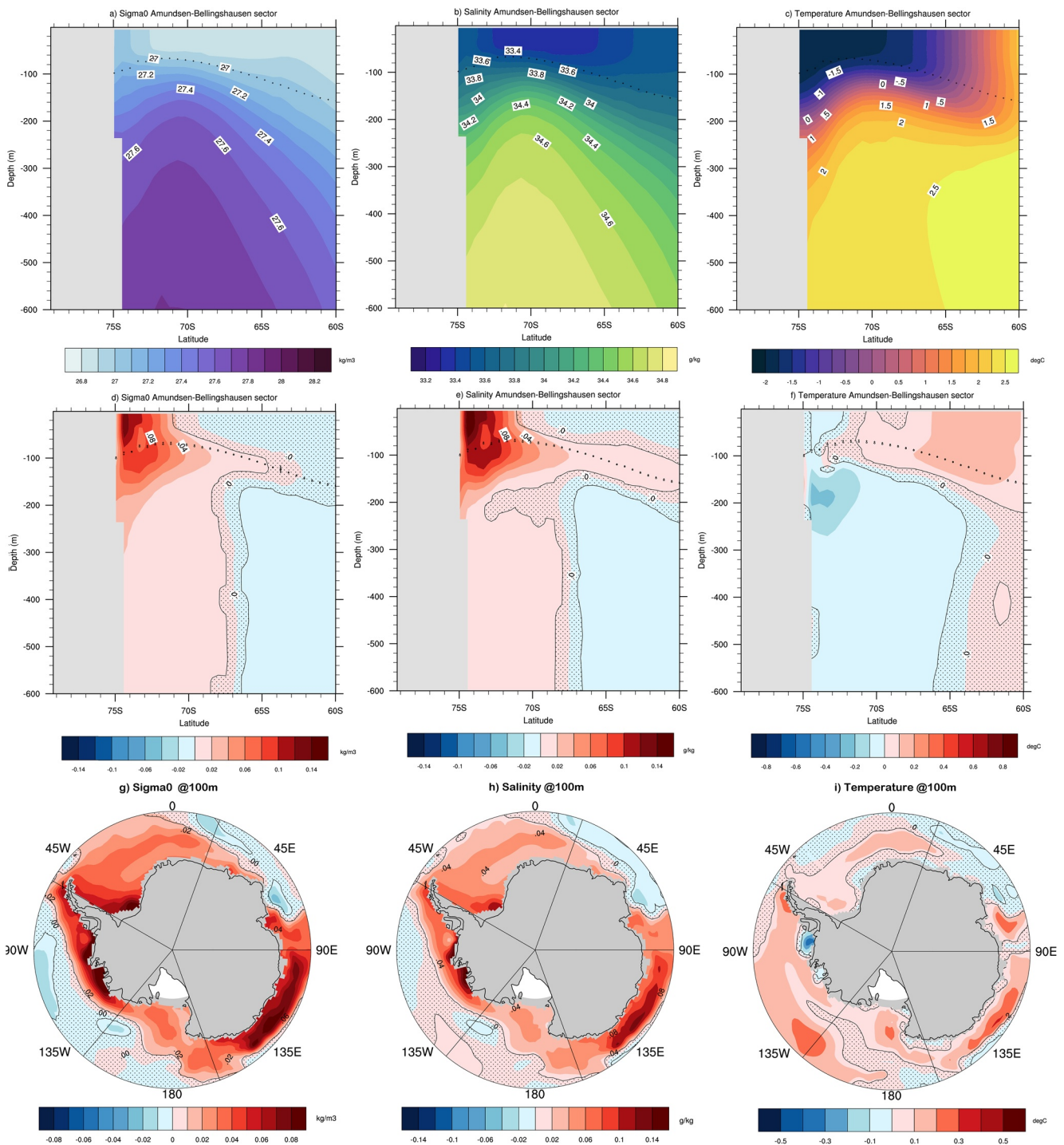


Figure 2. Winter (April-September) (a-c) mean and (d-f) transects averaged over the Amundsen-Bellingshausen sector, and (g-i) differences at 100 m depth for σ_0 (a, d, g; kg m^{-3}), salinity (b, e, h; g kg^{-1}), and temperature (c, f, i; $^{\circ}\text{C}$). All differences show MUSHY minus BL99 and regions that are significantly different at the 95% confidence level do not have stippling. For the transects, the MUSHY mixed layer depth is shown by plus symbols and the BL99 mixed layer depth is shown by open circles.

The impact of the differences in wintertime sea ice growth processes does not have a significant impact on summertime ocean chlorophyll levels. While the highest summertime chlorophyll levels occur in regions co-located with wintertime polynyas, the difference in chlorophyll over the top 100 m is insignificant between MUSHY and BL99 in most locations (Figure S12). At only two locations are chlorophyll levels

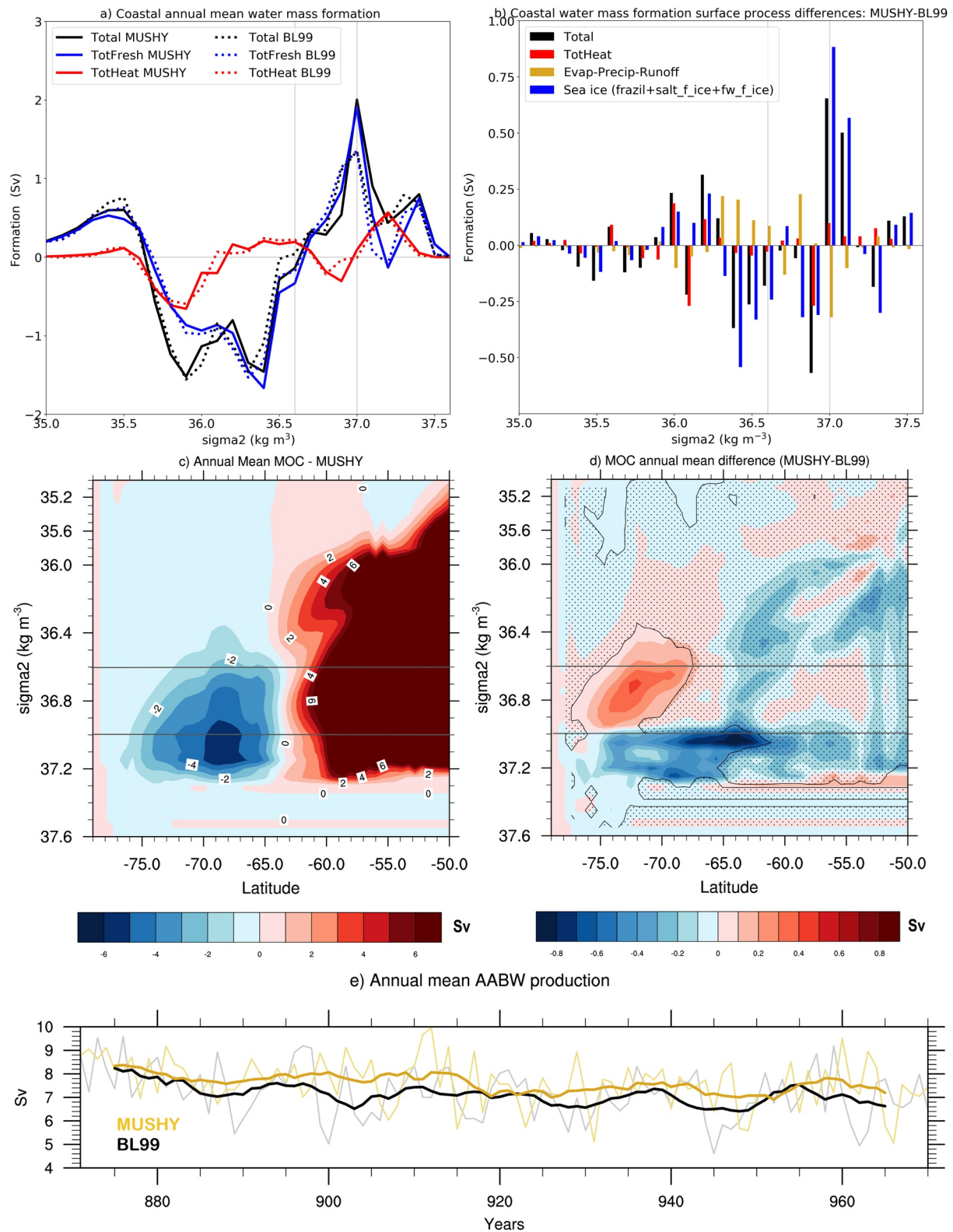


Figure 3.

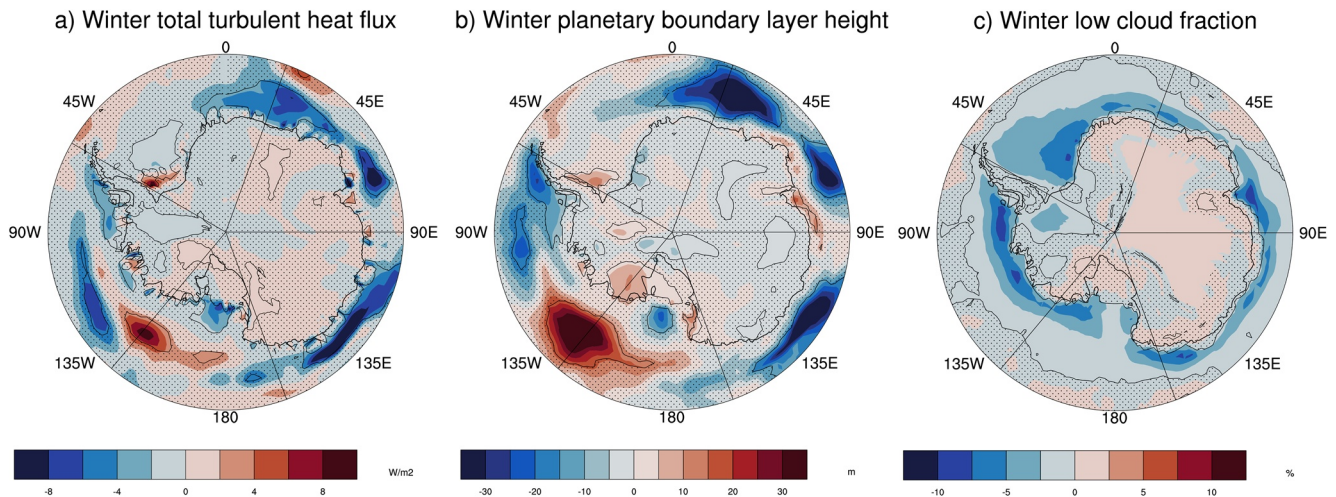


Figure 4. Winter (April-September) mean difference of (a) total turbulent heat flux (W m^{-2}), (b) atmospheric boundary layer height (m), and (c) winter cloud fraction (%). All differences show MUSHY minus BL99 and regions that are significantly different at the 95% confidence level do not have stippling.

significantly different and those are areas where the summertime ice state is significantly different (Figure S2). First, in the AB sector there is a decrease in chlorophyll that is co-located with significantly higher summertime sea ice concentration and thickness for MUSHY, and second, in the Indian Ocean sector there are significant increases in chlorophyll along the coast where the sea ice concentration and thickness are significantly lower in MUSHY.

3.3. Impacts on the Atmosphere

The impact of sea ice thermodynamics on the ocean are confined to the coastal areas and lower atmosphere. Along the Antarctic coasts, where there is slightly higher ice concentration and thickness in MUSHY (Figure S2), in MUSHY there are generally weaker turbulent heat fluxes (Figure 4a). The average decrease in turbulent heat flux is -3 W m^{-2} (-7% change), though the decrease in average fluxes in the Indian Ocean and Pacific Ocean sectors are -5.5 and -6.7 W m^{-2} (-11% change) respectively. The change in turbulent flux is driven primarily by changes in the sensible heat flux (Figure S13). This decrease in energy fluxed into the atmosphere leads to small but significant decreases in atmospheric planetary boundary height and low cloud cover near the Antarctic coasts (Figures 4b and 4c). Yet, there are not significant changes in winter-time sea level pressure (Figure S14a) or 500 hPa geopotential heights (not shown). Additionally, there are no significant differences along the coasts in near-surface temperature or moisture (Figures S14b and S14c). The significant differences in coastal precipitation and wind speed vary in sign and magnitude in different Antarctic sectors (Figures S14d and S14e), which suggests there is not a consistent impact of sea ice thermodynamics on these fields. Thus, while the MUSHY thermodynamics leads to local changes in atmospheric mixing and heat fluxes along the coast, on the whole it does not strongly impact the atmospheric circulation or drive consistent changes in precipitation.

While the majority of this study focuses on coastal impacts of sea ice thermodynamics, there are significant off-coast changes in the vicinity of the Amundsen Sea Low (Raphael et al., 2016) where the more sophis-

Figure 3. Coastal annual mean (a) MUSHY (solid lines) and BL99 (dashed lines) total surface water mass formation (Sv, black), total heat component (Sv, red), and total freshwater component (Sv, blue) and (b) difference (MUSHY minus BL99) in water mass formation for total formation (Sv, black), total heat term (Sv, red), total atmosphere and land freshwater components (Sv, gold), and total sea ice components (Sv, blue). Annual mean meridional overturning circulation (Sv) mapped to isopycnals for (c) MUSHY and (d) difference (MUSHY minus BL99) where values that are significantly different at the 95% confidence level do not have stippling. Gray lines on panels (a-d) at $\sigma_2 = 36.6 \text{ kg m}^{-3}$ and $\sigma_2 = 37.0 \text{ kg m}^{-3}$ indicate the densities of positive formation and Antarctic Bottom Water (AABW), respectively. (e) Timeseries of the BL99 (black) and MUSHY (gold) annual mean AABW formation (Sv); the yearly mean values are light while a 10 year running mean is indicated by the bold line.

ticated MUSHY thermodynamics experiment has significantly less ice cover (Figures S15a and S15b). The difference in the sea ice in this region is primarily due to early season differences in thermodynamic processes—specifically an increase in bottom melt and decrease in bottom growth in MUSHY (Figures S15c and S15d). However, there is no change in atmospheric circulation (Figure S14a), which is reflected in the lack of significant difference in sea ice dynamical changes (Figures S15c and S15d). Where the sea ice is less extensive, there are increased turbulent heat fluxes and planetary boundary layer heights (Figures 4a and 4b) as well as increased 2m Temperature and humidity (Figures S14b and S14c), and these are the result of the decrease in ice cover as more energy and moisture can enter the atmosphere with more open ocean water.

4. Discussion and Conclusions

This paper evaluates the impact of more realistic sea ice thermodynamics on the coupled Earth System. While there is not a large impact on the sea ice mean state, there are significant changes in both the processes that drive sea ice evolution and the coupled impacts on the ocean and atmosphere. With the more sophisticated MUSHY thermodynamics, all Antarctic sectors have a statistically significant increase in frazil and snow-ice growth that is partly compensated by decreases in bottom ice growth and increase in bottom melt throughout the ice growth season (Figure 1). It should be noted that bottom melt of newly formed ice throughout winter, as is seen in MUSHY, is not physically realistic and likely related to the limited representation of physical processes within the model. Increases in frazil ice are caused in part by the larger volume of ice created in MUSHY as well as increased dynamic loss in some sectors that would cause more open water. The increase in snow-ice formation is not related to changes in precipitation, which are insignificant and differ in sign across coastal locations. Instead, the increase in snow-ice growth is due partly to the larger volume of ice from flooding rather than compacting snow, and partly from the increase in bottom melt that would thin the ice and making it easier for snow to become submerged. The increase in sea ice bottom melt is likely related to higher internal sea ice salinity with a consequent higher liquid ice fraction.

The changes in the sea ice processes have a significant impact on the ocean state and MOC. Due to the larger volume of ice formed in MUSHY, there is more freshwater removal and the ocean becomes saltier and denser from the surface (Figure 2). However, the difference in freshwater removal between these experiments is due primarily to the limitations in ice-ocean coupling and prevents us from fully assessing realistic ice-ocean exchanges. In reality, the saltier ice in the MUSHY experiments would result in both salt being removed from the ocean in addition to freshwater, which would lessen the ocean water densification due to ice formation since more salt than 4 g kg^{-1} would be removed and this would balance some of the freshwater removal. Instead, our results are somewhat counter-intuitive: the more realistic sea ice physics in MUSHY results in both saltier sea ice and saltier ocean water since the salt content between the ice and ocean models are not directly exchanged. Instead, the ocean response to the more realistic sea ice thermodynamics depends only on the ice volume produced rather than the internal sea ice properties. While these ice-ocean coupling limitations are not unique to CESM2, understanding the implications as representation of sea ice physics improves and moves to a prognostic salinity is important for understanding coupled model behavior. Due in part to these results, we are actively working on implementing a true salt flux coupling in CESM2 that will account for realistic exchanges of both freshwater and salt between the ice and ocean.

In contrast to changes in salinity, there are minimal changes in the ocean temperature, particularly near the surface. Thus, the salinity changes primarily drive the changing ocean density. The water mass formation and MOC increase for densities $\sigma_2 = 37.0\text{--}37.2 \text{ kg m}^{-3}$ and $\sigma_2 = 37.4\text{--}37.5 \text{ kg m}^{-3}$, leading to a small, but significant, increase in AABW formation, while there is a decrease in formation for water densities $\sigma_2 = 36.4\text{--}36.9 \text{ kg m}^{-3}$ (Figure 3). Both changes are attributable to the sea ice processes. Because AABW is the densest water mass in the global oceans and an important component of the global thermohaline circulation, changes in this water mass due to sea ice thermodynamics have the potential for possible global impacts. Differences in coastal chlorophyll production are highly correlated with areas that have differences in summer sea ice state rather than changes in the ocean state (Figure S12).

The atmospheric impacts of sea ice thermodynamics are mostly confined to the Antarctic coasts. The more extensive and thicker coastal sea ice in MUSHY results in lower turbulent heat fluxes to the atmosphere. The lower energy input to the atmosphere leads to shallower atmospheric boundary layer depths, less atmospheric mixing, and decreased low-level cloud cover. Yet these coupled atmospheric effects are local and do not impact the large scale atmospheric circulation or state. There are not significant or consistent changes to atmospheric circulation, near surface winds, temperature, or humidity.

A number of questions remain. First, this study focuses on a preindustrial control experiment, but we can infer that in the future as the atmosphere and ocean warm the sea ice growth rates will decrease over time. Because sea ice processes are the dominant driver of surface water mass transformation, it would be expected that declining ice production might lead to decreases in AABW production. However, we find that more realistic sea ice physics leads to larger ice volume production, so future changes in AABW production may be delayed. Second, CESM2 simulations are relatively coarse in resolution. The CESM2 experiments are coarse resolution ($\sim 1^\circ$), yet coastal polynyas occur on small spatial scales that may require higher resolution to fully capture. Similarly, local wind impacts on polynyas, such as katabatic wind drainage, are not well resolved and likely underestimated in the CESM2 and this would impact dynamic loss and subsequent thermodynamic ice production. Additionally, while CESM2 uses a state-of-the-science sea ice model, CICE5, there are coastal processes such as the impact of ice tongues, fast-ice, or pancake ice formation that are not included as physical processes represented by CICE5, yet observations have shown these impact polynya formation (Thompson et al., 2020; Tison et al., 2020). Finally, we have used coastal ice production to imply the existence of polynyas, yet we find that the wintertime coastal monthly mean ice concentration is $\sim 100\%$. This may be due to using monthly data rather than daily data, which may be able to better identify short-lived polynya events, but further analysis with higher temporal frequency data is needed to understand polynya events. An outstanding question is how one should define a polynya, especially within a model where it is possible to have 100% ice concentration of thin ice that a satellite might still detect as open ocean and what the best methods are to compare with observations.

Data Availability Statement

Computing and data storage resources, including the Cheyenne supercomputer (<https://doi.org/10.5065/D6RX99HX>), were provided by the Computational and Information Systems Laboratory (CISL) at NCAR. Previous and current CESM versions are freely available online (at <https://www.cesm.ucar.edu/models/cesm2/>). The CESM data sets used in this study are freely available online from the NCAR Digital Asset Services Hub (at <https://doi.org/10.5065/bgt9-tz46>).

Acknowledgments

The CESM project is supported primarily by the National Science Foundation (NSF). This material is based upon work supported by the National Center for Atmospheric Research (NCAR), which is a major facility sponsored by the NSF under Cooperative Agreement 1852977. We thank all the scientists, software engineers, and administrators who contributed to the development of CESM2. M. M. Holland and L. Landrum acknowledge support from NASA grant 80NSSC20K1289. E. A. Maroon was supported by the Office of the Vice Chancellor for Research and Graduate Education at UW-Madison with funding from the Wisconsin Alumni Research Foundation. We would also like to thank two anonymous reviewers and the editor for their feedback that has improved this manuscript.

References

- Abernathy, R. P., Cerovecki, I., Holland, P. R., Newsom, E., Mazloff, M., & Talley, L. D. (2016). Water-mass transformation by sea ice in the upper branch of the Southern Ocean overturning. *Nature Geoscience*, 9(8), 596–601. <https://doi.org/10.1038/ngeo2749>
- Arrigo, K. R., & van Dijken, G. L. (2003). Phytoplankton dynamics within 37 Antarctic coastal polynya systems. *Journal of Geophysical Research*, 108(C8), 3271. <https://doi.org/10.1029/2002JC001739>
- Arrigo, K. R., van Dijken, G. L., & Strong, A. L. (2015). Environmental controls of marine productivity hot spots around Antarctica. *Journal of Geophysical Research: Oceans*, 120(8), 5545–5565. <https://doi.org/10.1002/2015JC010888>
- Assur, A. (1958). Arctic sea ice. *National Academy of Sciences-National Research Council. Chap. Composition of sea ice and its tensile strength*, 106–138.
- Bailey, D. A., Holland, M. M., DuVivier, A. K., Hunke, E. C., & Turner, A. K. (2020). Impact of sea ice thermodynamics in the CESM2 sea ice component. *Journal of Advances in Modeling Earth Systems*, 12, e2020MS002154. <https://doi.org/10.1029/2020MS002154>
- Bitz, C. M., & Lipscomb, W. H. (1999). An energy-conserving thermodynamic model of sea ice. *Journal of Geophysical Research*, 104(C7), 15669–15677. <https://doi.org/10.1029/1999JC900100>
- Bryan, F. O., Danabasoglu, G., Nakashiki, N., Yoshida, Y., Kim, D.-H., Tsutsui, J., & Doney, S. C. (2006). Response of the North Atlantic thermohaline circulation and ventilation to increasing carbon dioxide in CCSM3. *Journal of Climate*, 19(11), 2382–2397. <https://doi.org/10.1175/JCLI3757.1>
- Carrasco, J. F., Bromwich, D. H., & Monaghan, A. J. (2003). Distribution and characteristics of mesoscale cyclones in the Antarctic: Ross Sea eastward to the Weddell Sea. *Monthly Weather Review*, 131, 289–301. [https://doi.org/10.1175/1520-0493\(2003\)131<0289:DACOMC>2.0.CO;2](https://doi.org/10.1175/1520-0493(2003)131<0289:DACOMC>2.0.CO;2)
- Danabasoglu, G., Lamarque, J., Bacmeister, J., Bailey, D. A., DuVivier, A. K., Edwards, J., et al. (2020). The Community Earth System Model Version 2 (CESM2). *Journal of Advances in Modeling Earth Systems*, 12(2), e2019MS001916. <https://doi.org/10.1029/2019MS001916>
- Eicken, H. (1992). Salinity profiles of Antarctic sea ice: Field data and model results. *Journal of Geophysical Research*, 97(C10), 15545. <https://doi.org/10.1029/92JC01588>
- Fusco, G., Budillon, G., & Spezie, G. (2009). Surface heat fluxes and thermohaline variability in the Ross Sea and in Terra Nova Bay polynya. *Continental Shelf Research*, 29(15), 1887–1895. <https://doi.org/10.1016/j.csr.2009.07.006>

- Groeskamp, S., Griffies, S. M., Iudicone, D., Marsh, R., Nurser, A. G., & Zika, J. D. (2019). The water mass transformation framework for ocean physics and biogeochemistry. *Annual Review of Marine Science*, 11(1), 271–305. <https://doi.org/10.1146/annurev-marine-010318-095421>
- Handcock, M. S., & Raphael, M. N. (2020). Modeling the annual cycle of daily Antarctic sea ice extent. *The Cryosphere*, 14(7), 2159–2172. <https://doi.org/10.5194/tc-14-2159-2020>
- Hunke, E. C., Lipscomb, W. H., Turner, A. K., Jeffery, N., & Elliott, S. (2015). *CICE: The Los Alamos sea ice model documentation and software user's manual version 5*. (Tech. Rep.). Los Alamos, NM: Los Alamos National Laboratory.
- Karnovsky, N., Ainley, D., & Lee, P. (2007). The Impact and Importance of Production in Polynyas to Top-Trophic Predators: Three Case Histories. *Elsevier Oceanography Series* (Vol. 74, pp. 391–410). Elsevier. [https://doi.org/10.1016/S0422-9894\(06\)74012-0](https://doi.org/10.1016/S0422-9894(06)74012-0)
- Keen, A., Blockley, E., Bailey, D. A., Boldingh Debernard, J., Bushuk, M., Delhaye, S., et al. (2021). An inter-comparison of the mass budget of the Arctic sea ice in CMIP6 models. *The Cryosphere*, 15(2), 951–982. <https://doi.org/10.5194/tc-15-951-2021>
- Kern, S., & Aliani, S. (2011). A comparison between polynya area and associated ice production with mooring-based measurements of temperature, salinity and currents in the southwestern Ross Sea, Antarctica. *Annals of Glaciology*, 52(57), 291–300. <https://doi.org/10.3189/172756411795931705>
- Knuth, S. L., & Cassano, J. J. (2014). Estimating sensible and latent heat fluxes using the integral method from in situ aircraft measurements. *Journal of Atmospheric and Oceanic Technology*, 31(9), 1964–1981. <https://doi.org/10.1175/JTECH-D-14-00008.1>
- Labrousse, S., Fraser, A. D., Sumner, M., Tamura, T., Pinaud, D., Wienecke, B., et al. (2019). Dynamic fine-scale sea icescape shapes adult emperor penguin foraging habitat in East Antarctica. *Geophysical Research Letters*, 46(20), 11206–11218. <https://doi.org/10.1029/2019GL084347>
- Landrum, L., Holland, M. M., Schneider, D. P., & Hunke, E. (2012). Antarctic sea ice climatology, variability, and late twentieth-century change in ccsm4. *Journal of Climate*, 25(14), 4817–4838. <https://doi.org/10.1175/JCLI-D-11-00289.1>
- Large, W. G., & Nurser, A. G. (2001). Ocean surface water mass transformation. In G. Siedler, J. Church, & J. Gould (Eds.), *Ocean circulation and climate* (Vol. 77, pp. 317–336). Academic Press. [https://doi.org/10.1016/S0074-6142\(01\)80126-1](https://doi.org/10.1016/S0074-6142(01)80126-1)
- Massom, R. A., Harris, P., Michael, K. J., & Potter, M. (1998). The distribution and formative processes of latent-heat polynyas in East Antarctica. *Annals of Glaciology*, 27, 420–426. <https://doi.org/10.3189/1998AoG27-1-420-426>
- Mohrmann, M., Heuzé, C., & Swart, S. (2021). Southern ocean polynyas in CMIP6 models. *The Cryosphere Discussions*, 1–43. <https://doi.org/10.5194/tc-2021-23>
- Morales Maqueda, M. A. (2004). Polynya dynamics: A review of observations and modeling. *Reviews of Geophysics*, 42(1), RG1004. <https://doi.org/10.1029/2002RG000116>
- Nakata, K., Ohshima, K. I., & Nihashi, S. (2021). Mapping of active frazil for Antarctic coastal polynyas, with an estimation of sea-ice production. *Geophysical Research Letters*, 11, e2020GL091353. <https://doi.org/10.1029/2020GL091353>
- Newsom, E. R., Bitz, C. M., Bryan, F. O., Abernathy, R., & Gent, P. R. (2016). Southern ocean deep circulation and heat uptake in a high-resolution climate model. *Journal of Climate*, 29(7), 2597–2619. <https://doi.org/10.1175/JCLI-D-15-0513.1>
- Notz, D. (2005). *Thermodynamic and fluid-dynamical processes in sea ice*. University of Cambridge.
- Notz, D., & Worster, M. G. (2008). In situ measurements of the evolution of young sea ice. *Journal of Geophysical Research*, 113(C3), C03001. <https://doi.org/10.1029/2007JC004333>
- Raphael, M. N., Marshall, G. J., Turner, J., Fogt, R. L., Schneider, D., Dixon, D. A., et al. (2016). The Amundsen Sea low: Variability, change, and impact on Antarctic climate. *Bulletin of the American Meteorological Society*, 97(1), 111–121. <https://doi.org/10.1175/BAMS-D-14-00018.1>
- Singh, H. K. A., Landrum, L., Holland, M. M., Bailey, D., & DuVivier, A. (2020). An overview of Antarctic sea ice in the CESM2: Analysis of the seasonal cycle, predictability, and atmosphere-ocean-ice interactions. *Journal of Advances in Modeling Earth Systems*, 13, e2020MS002143. <https://doi.org/10.1029/2020MS002143>
- Speer, K., & Tziperman, E. (1992). Rates of water mass formation in the North Atlantic Ocean. *Journal of Physical Oceanography*, 22(1), 93–104. [https://doi.org/10.1175/1520-0485\(1992\)022<0093:ROWMFI>2.0.CO;2](https://doi.org/10.1175/1520-0485(1992)022<0093:ROWMFI>2.0.CO;2)
- Tamura, T., Ohshima, K. I., Fraser, A. D., & Williams, G. D. (2016). Sea ice production variability in Antarctic coastal polynyas. *Journal of Geophysical Research: Oceans*, 121(5), 2967–2979. <https://doi.org/10.1002/2015JC011537>
- Thompson, L., Smith, M., Thomson, J., Stammerjohn, S., Ackley, S., & Loose, B. (2020). Frazil ice growth and production during katabatic wind events in the Ross Sea, Antarctica. *The Cryosphere*, 14(10), 3329–3347. <https://doi.org/10.5194/tc-14-3329-2020>
- Tison, J.-L., Maksym, T., Fraser, A. D., Corkill, M., Kimura, N., Nosaka, Y., et al. (2020). Physical and biological properties of early winter Antarctic sea ice in the Ross Sea. *Annals of Glaciology*, 61, 241–259. <https://doi.org/10.1017/aog.2020.43>
- Turner, A. K., & Hunke, E. C. (2015). Impacts of a mushy-layer thermodynamic approach in global sea-ice simulations using the CICE sea-ice model. *Journal of Geophysical Research: Oceans*, 120(2), 1253–1275. <https://doi.org/10.1002/2014JC010358>
- Turner, A. K., Hunke, E. C., & Bitz, C. M. (2013). Two modes of sea-ice gravity drainage: A parameterization for large-scale modeling. *Journal of Geophysical Research: Oceans*, 118(5), 2279–2294. <https://doi.org/10.1002/jgrc.20171>
- Walin, G. (1982). On the relation between sea-surface heat flow and thermal circulation in the ocean. *Tellus*, 34(2), 187–195. <https://doi.org/10.1111/j.2153-3490.1982.tb01806.x>